JPE 1-2-4

An Improved Stationary Frame-based Digital Current Control Scheme for a PM Synchronous Motor

Kyeong-Hwa Kim* and Myung-Joong Youn

Dept. of Electrical Engineering, Korea Advanced Institute of Science and Technology
373-1, Kusong-Dong, Yusong-Gu, Taejon, 305-701, Korea

ABSTRACT

An improved stationary frame-based digital current control technique for a permanent magnet (PM) synchronous motor is presented. Generally, the stationary frame current controller is known to provide the advantage of a simple implementation. However, there are some unavoidable limitations such as a steady-state error and a phase delay in the steady-state. On the other hand, in the synchronous frame current regulator, the regulated currents are dc quantities and a zero steady-state error can be obtained through the integral control. However, the need to transform the signals between the stationary and synchronous frames makes the implementation of a synchronous frame regulator complex. Although the PI controller in the stationary frame gives a steady-state error and a phase delay, the control performance can be greatly improved by employing the exact decoupling control inputs for the back EMF, resulting in an ideal steady-state control characteristics irrespective of an operating condition as in the synchronous PI decoupling controller. However, its steady-state response may be degraded due to the inexact cancellation inputs under the parameter variations. To improve the control performance in the stationary frame, the disturbance is estimated using the time delay control. The proposed scheme is implemented on a PM synchronous motor using DSP TMS320C31 and the effectiveness is verified through the comparative simulations and experiments.

Key Words : Current control, stationary reference frame, PM synchronous motor, disturbance estimation, time delay control.

1. Introduction

PM synchronous motors have been gradually replacing DC motors in a wide range of drive applications such as machine tools and industrial robots. The advantage of using a PM synchronous motor is that many drawbacks caused by the brushes and commutators of a DC motor can be eliminated. Furthermore, the PM synchronous motor has the high power density, large torque to inertia ratio, and high efficiency as compared with a DC motor having the same output rating [1, 2]. The PM synchronous motor, however, has the nonlinear characteristics and inherent coupling problem. Therefore, to directly control the developed torque, the field-oriented control is usually employed. In the field-oriented control, the torque and flux producing components of the stator current vector are decoupled so that the independent torque and flux controls are possible as in DC motors. Thus, a high quality current control is essential for the successful implementation of the field-oriented control since the current controller has a direct influence on the drive performance [3, 4].

Manuscript received June 22, 2001; revised September 13, 2001.
Corresponding Author: khkim@rainbow.kaist.ac.kr, Tel: +82-42-869-8022, Fax: +82-42-869-3410

According to the reference frame in which a current controller is designed, the current control schemes for a voltage source inverter-fed PM synchronous motor drive system can be classified as two categories, namely, the stationary frame controller [4]-[7] and synchronous frame controller [8]-[13]. The hysteresis and ramp comparison controllers can be categorized into the stationary frame current controller. The synchronous PI decoupling regulator is designed in the synchronously rotating frame. On the other hand, the predictive control can be used in either reference frame. Generally, the stationary frame controller is known to provide the advantage of a simple implementation. However, there are some unavoidable limitations such as a steady-state current error and a phase delay in the steady-state since P or PI controller can not exactly track the sinusoidally varying reference and the back EMF acts as a disturbance in the current control loop [7, 8]. On the contrary, in the synchronous frame current regulator, the regulated currents are dc quantities. Thus, a zero steady-state error can be obtained through the use of an integral control. However, the need to transform the signals between the stationary and synchronous reference frames makes the implementation of a synchronous frame-based current regulator complex. Hence, a regulator with a zero steady-state error in the stationary frame would have an implementation advantage. First such an attempt is found in [7]. Although a zero steady-state error can be obtained by this control scheme, the transient performance seems to be unsatisfactory and the parameter variations have not been considered. Also, this scheme requires the speed informations for the regulator design. In view of the transient performance, however, it is more efficient to use the PI decoupling or predictive control using the speed informations [5, 6].

This paper presents an improved stationary frame-based digital current control scheme for a PM synchronous motor. Although the PI controller in the stationary frame gives a steady-state error and a phase delay, the control performance can be greatly improved by employing the exact decoupling control inputs for the back EMF and the PI control with a high bandwidth, resulting in an ideal steady-state control characteristics irrespective of operating conditions as in the synchronous PI decoupling controller. However, its steady-state response may be degraded due to the inexact cancellation inputs under the parameter variations such as the flux linkage, stator inductance, and stator resistance. Generally, it is very difficult to exactly obtain the informations on the machine parameters since they may vary during operation due to the changes in the temperature, current level, and operating frequency. In particular, the inaccuracy of the back EMF influences primarily on the control performance. This is more serious at high speed operation. In Ref. [13], to improve the control performance in the presence of the parameter variations, the time delay control has been applied to the synchronous frame current controller. The basic idea is to approximate a disturbance or uncertainty with the time-delayed value of control inputs and derivatives of state variables at the previous time step. This scheme can be an effective way for a control of systems with unknown dynamics and uncertainties since this algorithm does not require an explicit dynamic model nor does it depend on the estimation of specific parameters [14, 15]. Instead, it uses informations in the past to directly estimate the unknown dynamics or uncertainties at any given instant through the time delay. In this paper, this scheme will be employed for the estimation of the disturbance caused by the parameter variations to improve the steady-state control performance in the stationary frame-based digital current controller. The whole control system is realized by DSP TMS320C31 for a PM synchronous motor driven by a three-phase voltage-fed PWM inverter.

2. Modeling of a PM Synchronous Motor and Stationary Frame Current Control

A PM synchronous motor consists of permanent magnets mounted on the rotor surface and three phase stator windings which are sinusoidally distributed and displaced by 120°. The stator voltage equations of a PM synchronous motor in the stationary reference frame are described as follows [1]:

$$v_{qs} = R_s i_{qs} + L_s \dot{i}_{qs} + e_{qs} \tag{1}$$

$$v_{ds} = R_s i_{ds} + L_s \dot{i}_{ds} + e_{ds} \tag{2}$$

where R_s is the stator resistance, L_s is the stator inductance, and e_{qs} and e_{ds} represent the back EMF's.

These can be expressed as:

$$e_{qs} = \lambda_m \omega_r \cos\theta_r \tag{3}$$

$$e_{ds} = -\lambda_m \omega_r \sin\theta_r \tag{4}$$

where ω_r is the electrical rotor angular velocity, θ_r is the electrical rotor angular position, and λ_m is the flux linkage established by the permanent magnet.

The current references in the stationary reference frame can be obtained from those in the synchronously rotating reference frame using the relation as follows:

$$\begin{bmatrix} i_{qs}^* \\ i_{ds}^* \end{bmatrix} = \boldsymbol{K}(\theta_r) \begin{bmatrix} i_{qe}^* \\ i_{de}^* \end{bmatrix} \tag{5}$$

where $\boldsymbol{K}(\theta_r) = \begin{pmatrix} \cos\theta_r & \sin\theta_r \\ -\sin\theta_r & \cos\theta_r \end{pmatrix}$

subscript "s" denotes the quantities in the stationary reference frame, subscript "e" denotes the quantities in the synchronous reference frame, and the symbol "*" denotes the reference quantities. From the measurement of the phase currents, the current values in the stationary frame can be obtained as follows:

$$i_{qs} = i_{as} \tag{6}$$

$$i_{ds} = (i_{cs} - i_{bs})/\sqrt{3} \tag{7}$$

where i_{as}, i_{bs}, and i_{cs} denote the motor phase currents, respectively. Using the stationary frame PI controller for a current regulation, a steady-state current error and a phase delay are present in the phase currents since the back EMF's act as disturbances and the current references are varied sinusoidally. To improve the control performance, the control input voltages can be obtained using the PI decoupling control as follows:

$$v_{qs}^* = u_{qs} + e_{qs} \tag{8}$$

$$v_{ds}^* = u_{ds} + e_{ds} \tag{9}$$

where $u_{qs} = \left(K_P + \dfrac{K_I}{s}\right) \cdot (i_{qs}^* - i_{qs})$ (10)

$$u_{ds} = \left(K_P + \frac{K_I}{s}\right) \cdot (i_{ds}^* - i_{ds}) \tag{11}$$

s is the Laplace operator, and K_P and K_I are the proportional and integral gains, respectively. Then, the transfer function from i_{qs}^* to i_{qs} in the q-axis component of the stator current can be expressed as follows:

$$G_c(s) = \frac{i_{qs}(s)}{i_{qs}^*(s)} = \frac{K_P s + K_I}{L_s s^2 + (K_P + R_s)s + K_I} \tag{12}$$

If K_I is selected as $K_I = K_P R_s / L_s$, (12) reduces to

$$G_c(s) = \frac{\omega_c}{s + \omega_c} \tag{13}$$

where ω_c is the controller bandwidth expressed as $\omega_c = K_P / L_s$. The transfer function and controller bandwidth can be similarly obtained in the d-axis component of the stator current.

3. Disturbance Estimation Using Time Delay Control

From (1) and (2), the discrete-time equation of a PM synchronous motor can be obtained as follows:

$$\boldsymbol{v}_s(k) = \boldsymbol{A}\boldsymbol{i}_s(k) + \frac{L_s}{T}\boldsymbol{I} \cdot [\boldsymbol{i}_s(k+1) - \boldsymbol{i}_s(k)] + \boldsymbol{e}_s(k) \tag{14}$$

where $\boldsymbol{v}_s = [v_{qs} \quad v_{ds}]^T$, $\boldsymbol{i}_s = [i_{qs} \quad i_{ds}]^T$, $\boldsymbol{A} = R_s \boldsymbol{I}$

$$\boldsymbol{e}_s = \begin{bmatrix} e_{qs} \\ e_{ds} \end{bmatrix} = \begin{pmatrix} \lambda_m \omega_r(k)\cos[\theta_r(k)] \\ -\lambda_m \omega_r(k)\sin[\theta_r(k)] \end{pmatrix}, \ \boldsymbol{I} = \begin{pmatrix} 1 & 0 \\ 0 & 1 \end{pmatrix}$$

and T is a sampling period. Using the nominal parameters, (14) can be rewritten as follows:

$$\boldsymbol{v}_s(k) = \boldsymbol{A}_o \boldsymbol{i}_s(k) + \frac{L_{so}}{T}\boldsymbol{I} \cdot [\boldsymbol{i}_s(k+1) - \boldsymbol{i}_s(k)] + \boldsymbol{e}_{so}(k) + \boldsymbol{f}_s(k) \tag{15}$$

where $\boldsymbol{f}_s = [f_q \quad f_d]^T$, $\boldsymbol{A}_o = R_{so}\boldsymbol{I}$

$$\boldsymbol{e}_{so} = \begin{pmatrix} e_{qso} \\ e_{dso} \end{pmatrix} = \begin{pmatrix} \lambda_{mo}\omega_r(k)\cos[\theta_r(k)] \\ -\lambda_{mo}\omega_r(k)\sin[\theta_r(k)] \end{pmatrix}$$

subscript "o" denotes the nominal value, and $f_s(k)$ represents the disturbance vector caused by the parameter variations. This can be expressed as:

$$f_s(k) = \Delta A i_s(k) + \frac{\Delta L_s}{T} I \cdot [i_s(k+1) - i_s(k)] + \Delta e_s(k) \tag{16}$$

where $\Delta A = \Delta R_s I$, $\Delta e_s(k) = \begin{pmatrix} \Delta\lambda_m \omega_r(k)\cos[\theta_r(k)] \\ -\Delta\lambda_m \omega_r(k)\sin[\theta_r(k)] \end{pmatrix}$

$\Delta R_s = R_s - R_{so}$, $\Delta L_s = L_s - L_{so}$, and $\Delta\lambda_m = \lambda_m - \lambda_{mo}$.

The steady-state response of the stationary frame current control can be effectively improved by using a simple time delay control approach. In the time delay control, to obtain the estimates for the disturbance vector $f_s(t)$ in the continuous-time domain, it is considered that the value of $f_s(t)$ at the present time t is very close to that at time $t-\tau$ in the past for a small time delay τ as follows [13]-[15]:

$$f_s(t) \cong f_s(t-\tau) \tag{17}$$

In the discrete-time domain, (17) can be expressed as follows:

$$f_s(k) \cong f_s(k-L) \tag{18}$$

where $\tau = LT$ and L is a positive integer. Using (15) and (18), the simple estimates for the disturbance $f_s(k)$ can be derived as follows [13]:

$$\begin{aligned} \hat{f}_s(k) &\cong f_s(k-L) \\ &= v_s(k-L) - A_o i_s(k-L) \\ &\quad - \frac{L_{so}}{T} I \cdot [i_s(k-L+1) - i_s(k-L)] \\ &\quad - e_{so}(k-L) \end{aligned} \tag{19}$$

where $\hat{f}_s = [\hat{f}_q \;\; \hat{f}_d]^T$ and the symbol "^" denotes the estimated quantities. Although the unknown disturbance can be simply estimated by (19), this technique has some limitations. Since the numerical differentiation of the measured currents is needed for the estimation of $f_s(k)$, the high frequency noise in stator currents may be amplified. A low pass filter is employed to reduce this noise. This is done in a digital manner within a DSP. A simple first order low pass filter can be expressed in the continuous-time domain as follows:

$$G_f(s) = \frac{a}{s+a} \tag{20}$$

where a denotes the cut-off frequency of the low pass filter. For the digital implementation, (20) is discretized using the bilinear transform method where the Laplace operator s is replaced as follows [16]:

$$s = \frac{2}{T}\frac{1-z^{-1}}{1+z^{-1}}. \tag{21}$$

By substituting (21) into (20), the discrete-time transfer function of the low pass filter can be obtained as follows:

$$G_f(z) = \frac{\hat{f}_{qf}(z)}{\hat{f}_q(z)} = \frac{aT(1+z^{-1})}{(2+aT)-(2-aT)z^{-1}}. \tag{22}$$

Using (22), the filtered estimate for the q-axis disturbance can be obtained in a difference equation as follows:

$$\hat{f}_{qf}(k) = \frac{2-aT}{2+aT}\hat{f}_{qf}(k-1) + \frac{aT}{2+aT}[\hat{f}_q(k) + \hat{f}_q(k-1)] \tag{23}$$

Similarly, the filtered estimate for the d-axis disturbance can be obtained as follows:

$$\hat{f}_{df}(k) = \frac{2-aT}{2+aT}\hat{f}_{df}(k-1) + \frac{aT}{2+aT}[\hat{f}_d(k) + \hat{f}_d(k-1)] \tag{24}$$

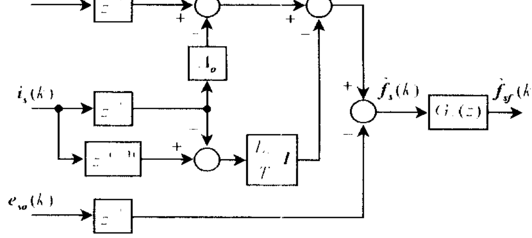

Fig. 1. Disturbance estimation using time delay control approach

Fig. 1 shows the proposed disturbance estimation scheme using the time delay control. The measured currents and voltages are delayed by L step and these delayed signals are used for the estimation of disturbances. Since this can be accomplished by only using the time delay of L step, some calculations, and low pass filter, the computational load of the controller is relatively small.

4. Stationary Frame Digital Current Control with Feedforward Disturbance Compensation

In the nominal conditions of $\boldsymbol{f}_s(k)=\mathbf{0}$, the stationary frame PI decoupling controller provides an ideal response irrespective of operating conditions. However, the motor parameters may vary during the operation mainly due to the temperature rise. Also, the exact modeling is generally very difficult. In these circumstances, $\boldsymbol{f}_s(k)$ is the function of the operating speed and current. The influences of such a disturbance on the current control performance are more serious at high speed operation under the variation of the flux linkage. The steady-state control performance of the stationary frame PI decoupling controller can be significantly improved through the use of a disturbance compensation technique, while retaining its good dynamic performance. By employing the estimated disturbances for a feedforward control, the reference voltage in the proposed stationary frame-based current regulator can be calculated as follows:

$$\boldsymbol{v}_s^*(k)=\boldsymbol{u}_s(k)+\boldsymbol{e}_{so}(k)+\hat{\boldsymbol{f}}_{sf}(k) \tag{25}$$

where $\hat{\boldsymbol{f}}_{sf}=[\hat{f}_{qf} \quad \hat{f}_{df}]^T$, $\boldsymbol{u}_s=[u_{qs} \quad u_{ds}]^T$, and u_{qs} and u_{ds} represent the PI controllers in (10) and (11), respectively. For the digital implementation, these controllers are discretized using the backward difference method as follows [16]:

$$u_{qs}(k)=u_{qs}(k-1)+K_P[e_{iq}(k)-e_{iq}(k-1)]+K_I Te_{iq}(k) \tag{26}$$

$$u_{ds}(k)=u_{ds}(k-1)+K_P[e_{id}(k)-e_{id}(k-1)]+K_I Te_{id}(k) \tag{27}$$

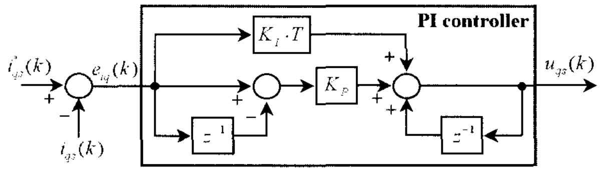

Fig. 2. Digital implementation for the q-axis PI controller using the backward difference method

where $e_{iq}(k)=i_{qs}^*(k)-i_{qs}(k)$ and $e_{id}(k)=i_{ds}^*(k)-i_{ds}(k)$

Then, the reference voltage is composed of the conventional PI decoupling control part and disturbance compensation part. Fig. 2 shows the digital implementation for the q-axis PI controller using the backward difference method.

5. Simulations and Experimental Results

In this section, the simulations and experimental results are presented to verify the feasibility of the proposed current control scheme under the various conditions. For the performance comparison with the proposed control scheme, the stationary frame PI control and PI decoupling control are employed. The overall block diagram for the proposed current control scheme is shown in Fig. 3. The overall system consists of a proposed current controller, a disturbance estimator using the time delay, a PWM inverter, and a PM synchronous motor. For the current control algorithm, the stationary frame PI decoupling control scheme with a feedforward disturbance compensation is used and the PI controllers are implemented in a digital manner as Fig. 2. By using this technique, the reference voltages are composed of the conventional PI decoupling control part and disturbance compensation part. During the operations, the disturbances caused by the parameter variations are estimated by using the time delay control approach and used for the feedforward control. The computed reference voltages are transformed to obtain the reference phase voltages using the relations as follows:

$$v_{as}^*=v_{qs}^* \tag{28}$$

$$v_{bs}^*=-(v_{qs}^*+\sqrt{3}v_{ds}^*)/2 \tag{29}$$

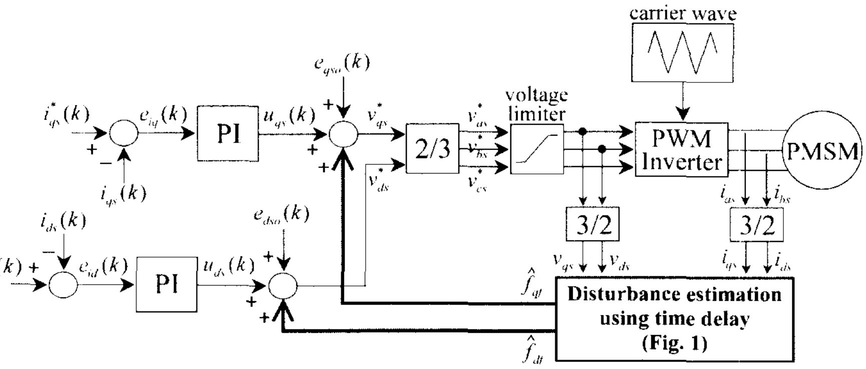

Fig. 3. Overall block diagram for the proposed current control scheme

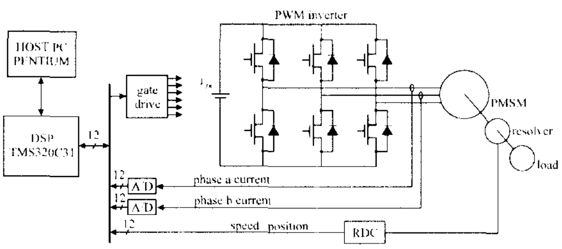

Fig. 4. Configuration of experimental system

$$v_{cs}^{*} = -(v_{qs}^{*} - \sqrt{3}v_{ds}^{*})/2 \tag{30}$$

These voltages are limited so that the conduction times of each switch cannot be in excess of the sampling time during large transient periods such as a starting and a sudden load change. The reference phase voltages are generated in the form of step waves at the positive peak of the carrier wave and are compared with the carrier wave to produce the drive signals for the inverter switches. Also, these reference phase voltages are fed into the disturbance estimator through the voltage limiter to be used for the feedback voltage for the disturbance estimation.

The configuration of the experimental system is shown in Fig. 4. The whole control algorithm is implemented using DSP TMS320C31 with a clock frequency of 40 MHz [17, 18]. The sampling period is set to 150 [μsec] both in the simulations and experiments. The PM synchronous motor is driven by a three-phase PWM inverter employing the intelligent power module (IPM) with a switching frequency of 6.67 kHz. The rotor speed and absolute rotor position are detected through a 12 bit/rev resolver-to-digital converter (RDC) using a brushless resolver. The current references in the stationary reference frame are obtained using (5) and the rotor position from an RDC.

Table 1. Specifications of a PM synchronous motor.

Rated power	400 W
Rated speed	3000 rpm
Rated torque	1.274 Nm
Number of poles	4
Magnetic flux	0.16 Wb
Stator resistance	3.0 Ω
Stator inductance	5 mH
Moment of inertia	1.54×10^{-4} Nm·s^2

The phase currents are detected by the Hall-effect devices and are converted to digital values through two 12-bit A/D converters, where the resolution of current is $7.4/2^{11}$ [A]. The detected phase currents are transformed to stationary dq currents using (6) and (7). The nominal parameters of a PM synchronous motor used for the simulations and experiments are listed in Table 1.

Fig. 5 shows the simulation results for the performance comparison of the stationary frame current controllers. The q-axis and d-axis current references are given as i_{qe}^{*}=2 [A] and i_{de}^{*}=0, respectively, and the motor is operated at a constant speed of 1500 [rpm]. The gains of the PI current controllers for the q-axis and d-axis are selected as K_p =20 and K_I =12000, respectively, so that the controller bandwidth is determined as ω_c =4000 [rad/sec].

Fig. 5(a) shows the current responses for the PI controller. It is shown that a steady-state current error and a phase delay are clearly present in the phase current responses. Fig. 5(b) shows the current responses for the PI decoupling controller.

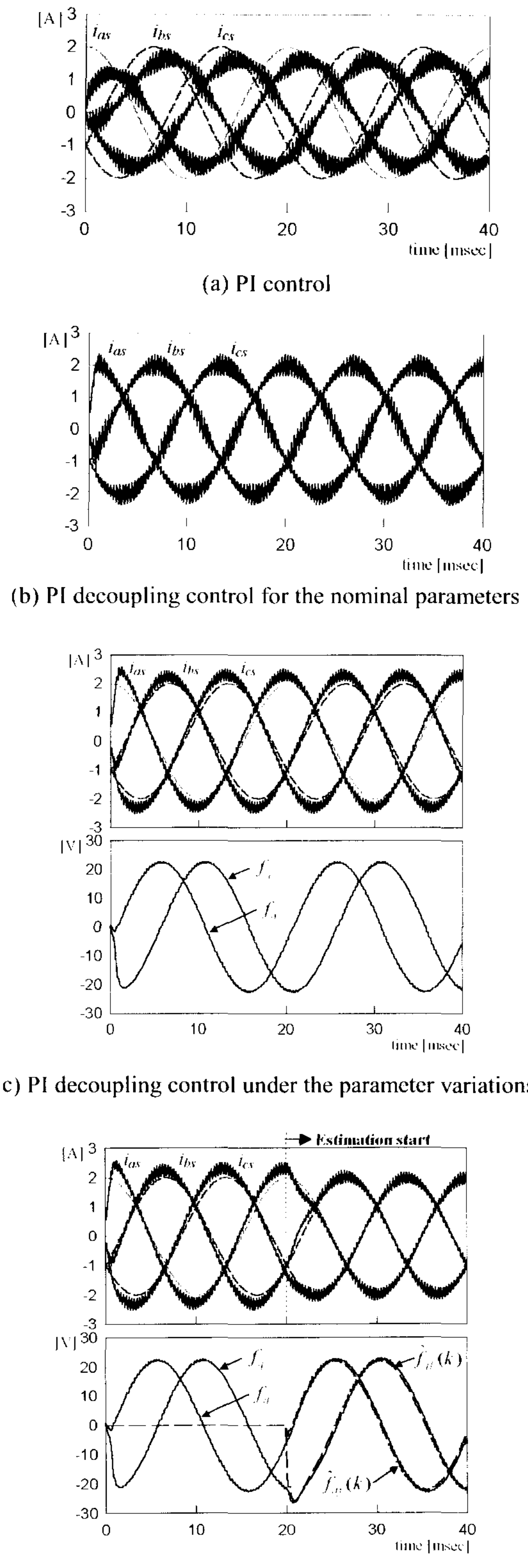

(a) PI control

(b) PI decoupling control for the nominal parameters

(c) PI decoupling control under the parameter variations

(d) Proposed control under the parameter variations

Fig. 5. Simulation results for the performance comparison of the stationary frame current controllers

As can be shown in this figure, in the nominal conditions of $f_s(k)=\mathbf{0}$, the PI decoupling controller in the stationary frame can give an ideal response irrespective of operating condition.

Fig. 5(c) shows the current responses for the PI decoupling controller under the parameter variations ($\Delta\lambda_m = -0.5\lambda_{mo}$, $\Delta L_s = 1.0 L_{so}$, and $\Delta R_s = 1.0 R_{so}$). Even though an ideal characteristics can be obtained for the nominal parameter values, the steady-state current error is observed in the phase currents under the parameter variations. This is caused by the sinusoidally-varying disturbance voltages due to the parameter variations as can be shown in Fig. 5(c). This degradation is expected to be more serious at high speed operation because the magnitude of the disturbance is proportional to an operating speed. Fig. 5(d) shows the simulation result for the proposed control scheme under the same parameter variations as Fig. 5(c). Before the estimation algorithm starts, the steady-state errors are observed in the phase currents. However, as soon as the estimation algorithm starts at t=20 [msec] and the estimated disturbances are used for a feedforward control, the steady-state current errors and phase delays are quickly removed within a few milliseconds. This can be explained by the estimation of the disturbance voltages as shown in this figure. For the design of the time-delayed disturbance estimator, L=1 is chosen. Also, a=2000 is selected for the cut-off frequency of the low pass filter, which corresponds to the cut-off frequency of 318 Hz. Since the maximum electrical frequency of the used PM synchronous motor is 100 Hz and the inverter switching frequency is 6.67 kHz, the high frequency noise caused by inverter switching can be well suppressed without affecting any influences on the fundamental current component.

Fig. 6 shows the comparison of the transient responses for the a-phase current under the step change in the current command. For the performance comparison with the proposed control scheme, the PI decoupling control, the predictive plus time delay control in the synchronous frame [13], and the predictive plus time delay control in the stationary frame are employed. In all simulation results, the same parameter variations as Fig. 5 are assumed and the motor is operated at 1500 [rpm].

In Fig. 6(a) and (c), the bandwidths for the PI controllers are selected as ω_c =4000 [rad/sec], respectively.

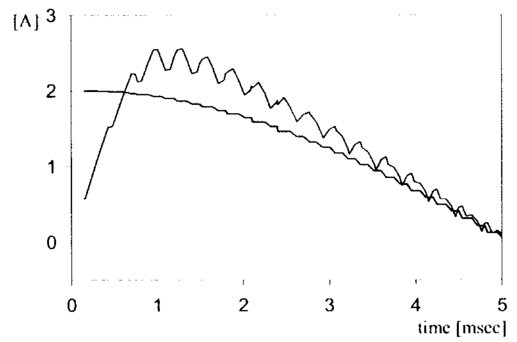

(a) PI decoupling control in synchronous frame

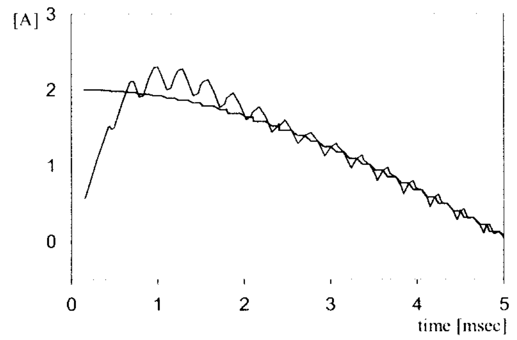

(b) Predictive plus time delay estimator in synchronous frame [Ref. 13]

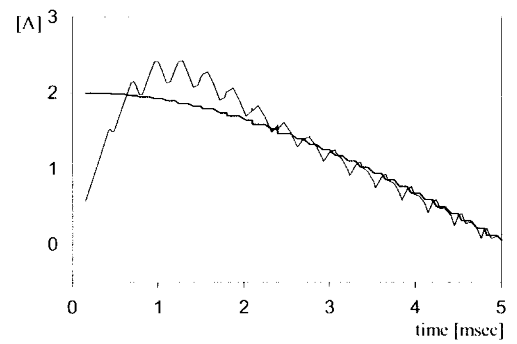

(c) Proposed control

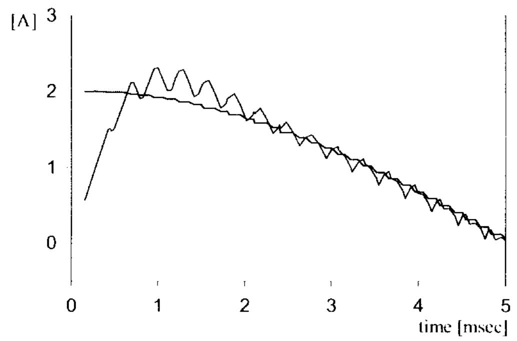

(d) Predictive plus time delay estimator in stationary frame

Fig. 6. Comparison of the transient response for the a-phase current under the step change in current command

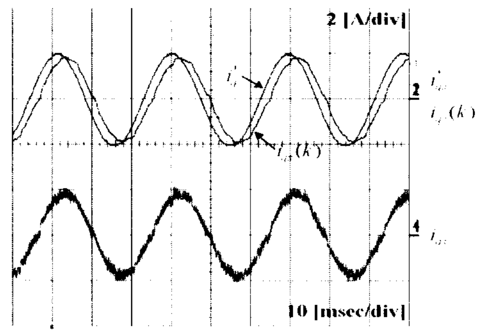

(a) PI control

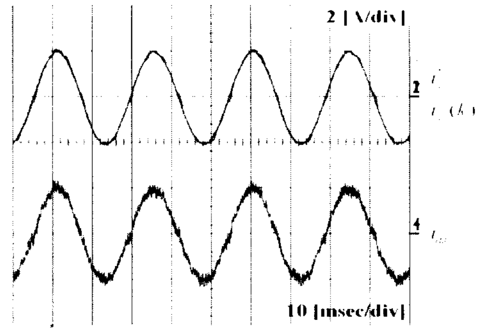

(b) PI decoupling control for the nominal parameters

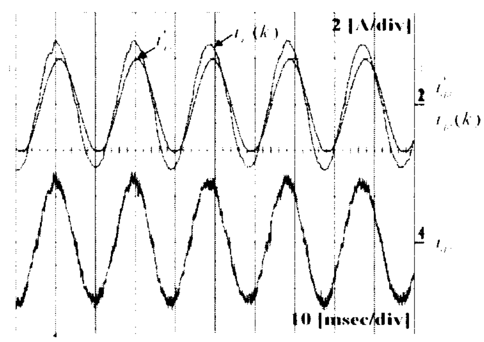

(c) PI decoupling control under $\Delta\lambda_m = -0.5\lambda_{mo}$

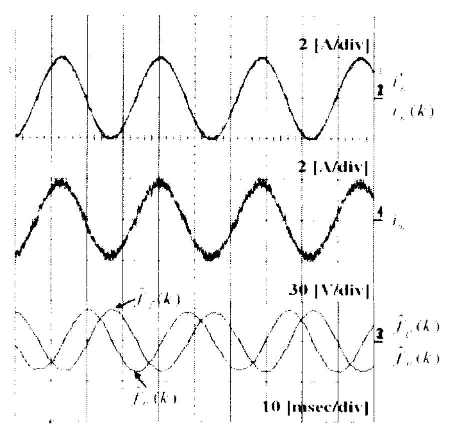

(d) Proposed control under $\Delta\lambda_m = -0.5\lambda_{mo}$

Fig. 7. Experimental results for the performance comparison

Also, for the time-delayed disturbance estimator, L=1 and a=2000 are chosen in Fig. 6(b), (c), and (d). As can be shown in Fig. 6(a), the PI decoupling control in the synchronous frame gives somewhat slow transient and larger overshoot under the parameter variations although it provides an ideal steady-state response through the use of an integrator. The control scheme in Ref. [13] and the stationary frame predictive plus time delay control yield the best transient response with a smaller overshoot. The transient performance of the proposed control scheme in Fig. 6(c) lies between the synchronous PI decoupling control and the control scheme in Ref.[13]. However, since the proposed scheme is implemented in the stationary reference frame, some computational load can be reduced in the controller.

Fig. 7 shows the experimental results of the stationary frame current controllers for the performance comparison. The q-axis and d-axis current references are given as i^*_{qe}=2 [A] and i^*_{de}=0, respectively. Also, the experiments are carried out under the same conditions as the simulations in Fig. 5. Fig. 7(a) shows the result for the PI controller. Fig. 7(b) and (c) show the control performance for the PI decoupling controller under the nominal parameters and under $\Delta\lambda_m = -0.5\lambda_{mo}$, respectively. Fig. 7(d) shows the current responses and estimated disturbances for the proposed control scheme and the all experimental results are shown to be well coincided with the simulation results of Fig. 5.

Fig. 8 shows the experimental results when i^*_{qe} is changed from 1 [A] to 2 [A] under $\Delta\lambda_m = -0.5\lambda_{mo}$. In the PI decoupling control, the error in $i_{qs}(k)$ becomes larger since the magnitude of the disturbance is increased as the rotor speed is increased. In the proposed control scheme, however, $i_{qs}(k)$ is well controlled to its reference irrespective of the operating speed and current level through the use of an effective disturbance estimation scheme.

6. Conclusions

An improved stationary frame-based digital current control scheme for a PM synchronous motor using the time delay control approach is presented. Although the PI controller in the stationary frame gives a steady-state error and a phase delay, the control performance can be greatly improved by employing the exact decoupling control inputs for the back EMF and the PI control with a high bandwidth, resulting in an ideal steady-state control characteristics irrespective of operating conditions as in the synchronous PI decoupling controller. However, its steady-state response may be degraded due to the inexact cancellation inputs under the inexact motor modeling or some parameter variations such as the flux linkage, stator inductance, and stator resistance. Generally, it is very difficult to exactly obtain the informations on the machine parameters since they may vary during operation due to

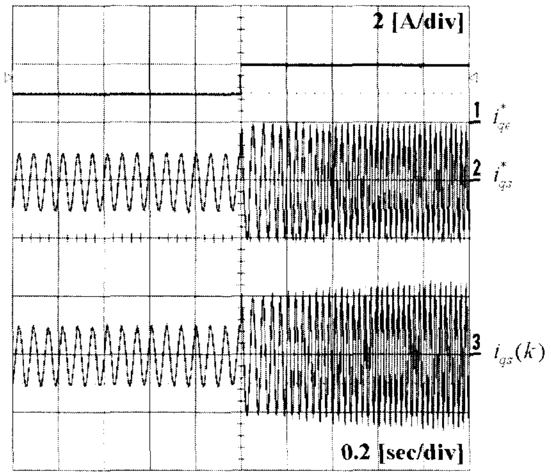

(a) PI decoupling control

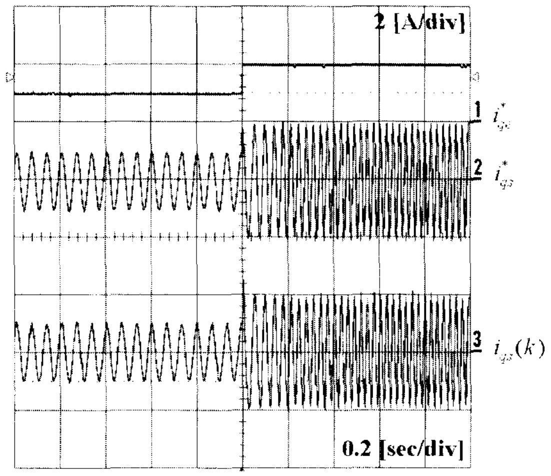

(b) Proposed control

Fig. 8. Experimental results for the step change in i^*_{qe} under $\Delta\lambda_m = -0.5\lambda_{mo}$

the changes in the temperature, current level, and operating frequency. This is more serious at high speed under the flux linkage variation since the disturbance is proportional to an operating speed. To improve the current control performance in the stationary frame, the disturbance caused by the parameter variations is estimated by using a time delay control and the estimated disturbance is used for the computation of the reference voltages by a feedforward manner. The design procedures are straightforward and the current control performance is not affected by the variation of the motor parameters and operating conditions. The whole control algorithm is implemented using DSP TMS320C31 for a PM synchronous motor driven by a three-phase voltage-fed PWM inverter and the effectiveness is verified through the comparative simulations and experiments. As a result, an ideal and a stable control performance can be obtained in the stationary reference frame.

References

[1] P. C. Krause, *Analysis of Electric Machinery*. New York: McGraw-Hill, 1986.

[2] T. H. Liu, C. M. Young, and C. H. Liu, "Microprocessor-based controller design and simulation for a permanent magnet synchronous motor drive," *IEEE Trans. Ind. Electron.*, vol. 35, no. 4, pp. 516~523, Nov. 1988.

[3] D. W. Novotny and R. D. Lorenz, *Introduction to field orientation and high performance AC drives*. *IEEE* IAS Tutorial Course, 1986.

[4] D. M. Brod and D. W. Novotny, "Current control of VSI-PWM inverters," *IEEE Trans. Ind. Applicat.*, vol. 21, no. 4, pp. 562~570, May/Jun. 1985.

[5] H. L. Huy and L. A. Dessaint, "An adaptive current control scheme for PWM synchronous motor drives: Analysis and simulation," *IEEE Trans. Power Electron.*, vol. 4, no. 4, pp. 486~495, Oct. 1989.

[6] L. Ben-Brahim and A. Kawamura, "Digital control of induction motor current with deadbeat response using predictive state observer," *IEEE Trans. Power Electron.*, vol. 7, no. 3, pp. 551~559, Jul. 1992.

[7] D. N. Zmood, D. G. Holmes, and G. H. Bode, "Frequency-domain analysis of three-phase linear current regulators," *IEEE Trans. Ind. Applicat.*, vol. 37, no. 2, pp. 601~610, Mar./Apr. 2001.

[8] T. M. Rowan and R. J. Kerkman, "A new synchronous current regulator and an analysis of current-regulated PWM inverters," *IEEE Trans. Ind. Applicat.*, vol. 22, no. 4, pp. 678~690, Jul./Aug. 1986.

[9] D. S. Oh, K. Y. Cho, and M. J. Youn, "A discretized current control technique with delayed input voltage feedback for a voltage-fed PWM inverter," *IEEE Trans. Power Electron.*, vol. 7, no. 2, pp. 364~373, Apr. 1992.

[10] D. C. Lee, S. K. Sul, and M. H. Park, "High performance current regulator for a field-oriented controlled induction motor drive," *IEEE Trans. Ind. Applicat.*, vol. 30, no. 5, pp. 1247~1257, Sep./Oct. 1994.

[11] L. Zhang, R. Norman, and W. Shepherd, "Long-range predictive control of current regulated PWM for induction motor drives using the synchronous reference frame," *IEEE Trans. Contr. Syst. Technol.*, vol. 5, no. 1, pp. 119~126, Jan. 1997.

[12] K. H. Kim, I. C. Baik, and M. J. Youn, "An improved digital current control of a PM synchronous motor with a simple feedforward disturbance compensation scheme," in *Proc. IEEE Int. Conf. PESC'98*, 1998, pp. 101~107.

[13] K. H. Kim and M. J. Youn, "A simple and robust digital current control technique of a PM synchronous motor using time delay control approach," *IEEE Trans. Power Electron.*, vol. 16, no. 1, pp. 72~82, Jan. 2001.

[14] K. Youcef-Toumi and O. Ito, "A time delay controller for systems with unknown dynamics," *ASME J. Dyn. Sys., Meas., Contr.*, vol. 112, pp. 133~142, Mar. 1990.

[15] P. H. Chang and J. W. Lee, "A model reference observer for time-delay control and its application to robot trajectory control," *IEEE Trans. Contr. Syst. Technol.*, vol. 4, no. 1, pp. 2~10, Jan. 1996.

[16] K. Ogata, *Discrete-time Control Systems*. Prentice-Hall, 1987.

[17] *TMS320C3x User's Guide*, Texas Instrument, 1990.

[18] *TMS320C30 Assembly Language Tools User's Guide*, Texas Instrument, 1990.

Kyeong-Hwa Kim was born in Seoul, Korea, in 1969. He received the B.S. degree in electrical engineering from Hanyang University, Seoul, Korea, in 1991, and the M.S. and Ph.D. degrees in electrical engineering from the Korea Advanced Institute of Science and Technology (KAIST), Taejon, Korea, in 1993 and 1998, respectively. From 1998 to 2000, he was a Research Engineer with Samsung Electronics Company, where he was engaged in research of motor drive systems. Since July 2000, he has been with KAIST, Taejon, Korea, where he is currently an invited research professor. His current research interests are in the areas on power electronics, ac machine drives, and DSP-based control applications.

Myung-Joong Youn was born in Seoul, Korea on November 26, 1946. He received the B.S. degree from Seoul National University, Seoul, Korea in 1970 and the M.S. and Ph.D. degrees in electrical engineering from the University of Missouri-Columbia in 1974 and 1978, respectively. He was with the Aircraft Equipment Division of General Electric Company at Erie, Pennsylvania, since 1978, where he was an Individual Contributor on Aerospace Electrical Engineering. He has been with the Korea Advanced Institute of Science and Technology since 1983 where he is now a professor. His research activities are in the areas on power electronics and control, which include the drive system, rotating electrical machine design, and high performance switching regulators. Prof. Youn is a member of the KIPE, KIEE, and IEEK.